

# Multi-objectivization-based Localization of Underwater Sensors Using Magnetometers

Zhou Yu, Changhan Xiao, and Guohua Zhou

**Abstract**—Underwater sensor networks (USNs) are necessary to detect and track unknown targets in the maritime environment. Localization of sensors becomes a crucial problem. This research presents a new method based on multi-objectivization to localize the sensors using triaxial magnetometers. In this localization system, a DC current-carrying solenoid coil serves as a magnetic source and the inertial magnetometer measure the three-component of magnetic flux intensity. Then the localization problem is translated into a multi-objective optimization problem by minimizing each error function. Without using depth sensor, it is difficult to find the global optimum of the functions due to the homogeneous magnetic field. Accordingly, we propose a hybrid algorithm using improved Non-dominated Sorting Genetic Algorithm (NSGA-IIb) and linear multi-metering method to determine the sensor position. In order to reduce time consumption during the optimization process, a simplified discrete model of the magnetic field is derived. Experiment results show that the proposed localization method has a high accuracy and strong robustness.

**Index Terms**—Underwater sensor, localization, multi-objectivization, magnetometer.

## I. INTRODUCTION

AN underwater sensor network is necessary to track and identify passing targets. Several methods are proposed based on different principles, for example, magnetic, acoustic, electric or optical. By sensing several physical properties, such as the magnetic, electric field disturbances and noises caused by the vessel, the relative position between the sensor and target is determined. Due to extreme oceanic conditions and complications of engineering practice, deploying an underwater magnetometer sensor in its predetermined position is difficult. Especially, currents and surge may also move the sensors. Without correct sensor positions, accurately tracking of targets becomes impossible. Sensor positions must be localized before the measurement.

The localization of underwater sensors is a challenging scheme and has attracted significant interest recently. Several localization solutions have been suggested for terrestrial sensor networks (TSNs), yet they are not suitable for USNs [1]. TSNs generally acquire their positions in advance using global navigation satellite systems (GNSS) (e.g.

GPS). Unfortunately, the GNSS signals are not accessible or too weak to be detected in scenarios such as indoor or underground venues. Additionally, the high frequency radio waves are severely absorbed by the water. Radio signal propagates at long distances through sea water only at extra low frequencies, which causes high energy consumption and extra cost. Acoustic signals attenuate less and travel further distances than radio signals and optical signals. Consequently, acoustic communication emerges as a choice for underwater communications [2], [3]. There are two categories of the localization schemes: range-based schemes and range-free schemes. Range-base schemes estimate the locations of sensors by using inter-sensor measurements and the prior knowledge of the locations of a few reference sensors. So they can provide more accurate localization compared to range-free schemes [4]-[7]. To avoid the cost of ranging, range-free techniques have been proposed [8]-[11]. They demand no extra devices and rely solely on connectivity information. More details of the underwater acoustic sensor networks (UASNs) are available in [12] and [13].

Due to the irreplaceable role and the fragility of the USNs in military applications, localization systems can be a target of an attack, which could lead incorrect military plans and decision making. Security techniques are required to prevent or impede such attacks. In UASNs, there are two kinds of message communication: silent and active. Silent localization techniques may preserve the anonymity of the underwater sensor nodes. They also have lower energy consumption and communication overhead. Localization with Directional Beacons is proposed as a silent positioning technique for UASNs [14]. Dive and rise localization protocol is also suggested by utilizing a large number of mobile anchor nodes, which are able to descent and ascent [15]. Underwater positioning scheme is a time difference of arrival (TDOA)-based localization scheme [16]. It requires four fixed anchors with known positions.

Comparatively, silent localization using magnetometers (SLM) method is more useful in a shallow maritime environment with the advantage of energy efficiency, low cost and ignorable scatterance. They are assumed to send data via wired communications. In military researches and medical services, magnetic localization methods are applied to magnetic objective tracking and detection. A small permanent magnet can be modelled as a point magnetic dipole at distances more than three times the target largest dimensions [17]. Several studies modelled ferromagnetic by using a multipole model [18], [19]. A magnetic sensor array must be placed in specific spatial points in order to identify, localize, and track ferromagnetic targets. Then appropriate

Manuscript received July 2, 2013; revised August 21, 2013; accepted October 10, 2013. Date of publication November 1, 2013; date of current version December 10, 2013. The associate editor coordinating the review of this paper and approving it for publication was XXX.

Z. Yu, C.H. Xiao, and G.H. Zhou are with the Electrical Engineering Department, Naval University of Engineering, Wuhan, 430033 China. (e-mail: zhouyujoeh@163.com; xiaochanghan@163.com; dandanqibing@126.com).

Color versions of one or more of the figures in this paper are available online at <http://ieeexplore.ieee.org>.

Digital Object Identifier 10.1109/JSEN.2013.XXXXXX

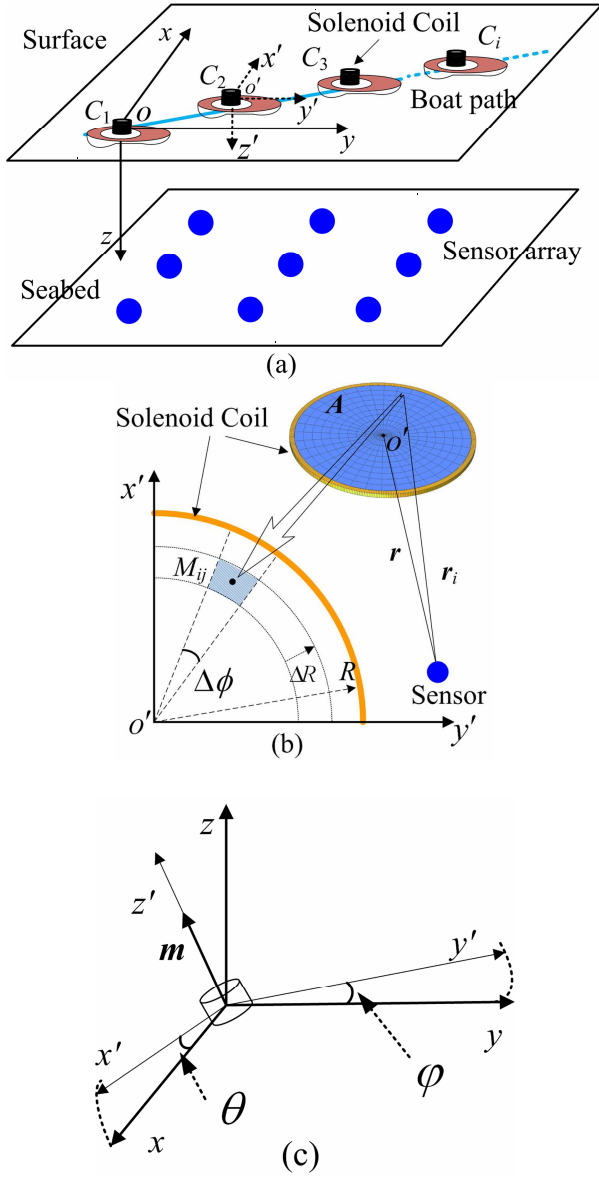


Fig. 1. (a) The Arrangement of the Coil and the Underwater Sensor Array; (b) The Discretization of the Coil Loop; (c) Coil Orientation.

optimization algorithms, such as Levenberge-Marquardt (LM) method [20]-[22] and particle swarm optimization (PSO) algorithm[23], are used to minimize the objective function obtained from the measured sensor data. The localization of sensors is to solve the inverse problem. A silent method was explored to localize underwater sensors equipped with triaxial [24]. It used an extended Kalman Filter and a friendly vessel with known static magnetic characteristics. By the use of depth sensors, the 3D position problem was simplified into a 2D problem, and yet it increases the cost. Another suggested localization method equipped one of the underwater magnetometer sensors with an electric solenoid [25]. Since dimensions (e.g. coil radius, number of windings) are fixed, the coil cannot be optimized according to the range condition. It also causes accumulated error for the location of other sensors.

In this paper, we propose a simple and convenient localization algorithm based on multi-objectivization technique. Firstly, a solenoid coil carrying direct current is designed as a magnetic source and carried by a boat. The

solenoid coil moves along a predetermined trajectory above the sensor field. Simultaneously, the magnetometers in the underwater sensors measure the magnetic field and return the collected data. Using the measured magnetic vectors, the localization problem is translated into a multi-objective optimization problem. Through an improved non-dominated sorting genetic algorithm and correction method, the sensor positions are determined.

The outline of the paper is as follows. In Section II, we introduce a discrete mathematical model of the magnetic field. In Section III, we present the localization algorithm of magnetometer sensors based on multi-objectivization, which is followed by the experimental results and analysis in Section IV. Finally, we conclude the paper in Section V.

## II. DISCRETE MODEL

Fig. 1 (a) presents the sensor arrangement and coil setup. The center of the coil is set as the origin  $o'$  of the coil coordinate system  $o'-x'y'z'$  and the first coil location  $C_1$  is set as the origin  $o$  of the global coordinate system  $o-xyz$ . In the coil coordinates, the magnetic flux density  $B' = [B'_x, B'_y, B'_z]^T$  at the sensor position ( $P' = [p_x, p_y, p_z]^T$ ) generated by the coil can be derived as follows[26]:

$$B'(P', C) = \frac{\mu_0 N_w I}{2\pi \sqrt{(\sqrt{p_x^2 + p_y^2} + R)^2 + p_z^2}} \times \left\{ \frac{p_x p_z}{p_x^2 + p_y^2} \left[ \frac{r^2 + R^2}{\sqrt{(\sqrt{p_x^2 + p_y^2} - R)^2 + p_z^2}} E(k) - K(k) \right] e'_x + \frac{p_y p_z}{p_x^2 + p_y^2} \left[ \frac{r^2 + R^2}{\sqrt{(\sqrt{p_x^2 + p_y^2} - R)^2 + p_z^2}} E(k) - K(k) \right] e'_y + \left[ \frac{R^2 - r^2}{\sqrt{(\sqrt{p_x^2 + p_y^2} - R)^2 + p_z^2}} E(k) + K(k) \right] e'_z \right\} \quad (1)$$

where  $N_w$  is the number of windings,  $R$  is the coil radius,  $I$  is the direct current applied,  $\mu_0$  is the magnetic permeability of vacuum,  $r$  is the distance between the sensor position  $P'$  and the coil center  $C$ ,  $e'_x$ ,  $e'_y$  and  $e'_z$  are the base vectors of the coil coordinates system, and

$$k^2 = 4R\sqrt{p_x^2 + p_y^2} / \left[ (\sqrt{p_x^2 + p_y^2} + R)^2 + p_z^2 \right] \quad (2)$$

$$K(k) = \int_0^{\pi/2} \frac{d\alpha}{\sqrt{1 - k^2 \sin^2 \alpha}}$$

$$E(k) = \int_0^{\pi/2} \sqrt{1 - k^2 \sin^2 \alpha} d\alpha$$

In the process of iterative optimization, calculating the elliptic integrals show in (2) for every step is extremely time-consuming. If the distance  $r$  is large enough in comparison with coil radius  $R$ , the solenoid coil can be simplified as a magnetic dipole resulting in:

$$\mathbf{B}_d = \frac{\mu_0 \mathbf{m}}{4\pi(p_x^2 + p_y^2 + p_z^2)^{\frac{5}{2}}} \begin{bmatrix} 3p_x p_z \\ 3p_y p_z \\ 2p_z^2 - p_x^2 - p_y^2 \end{bmatrix} \quad (3)$$

Here,  $\mathbf{m}$  is the dipole moment.  $\mathbf{m} = N_w I \mathbf{A}$ ,  $A$  is the coil area. We can mesh the inner coil region into a number of small elements if the calculated spatial point is closed to the coil (Fig. 1 (b)). Then the coil loop can be thought of being composed of many dipoles. The magnetic field produced by coil can be calculated directly by summing the contribution from each dipole:

$$\mathbf{B}_d = \sum_{i=1}^{n_1} \sum_{j=1}^{n_2} \frac{\mu_0 N_w I \mathbf{A}_{ij}}{4\pi[(p_x - x_{ij})^2 + (p_y - y_{ij})^2 + p_z^2]^{\frac{5}{2}}} \times \begin{bmatrix} 3(p_x - x_{ij})p_z \\ 3(p_y - y_{ij})p_z \\ 2p_z^2 - (p_x - x_{ij})^2 - (p_y - y_{ij})^2 \end{bmatrix} \quad (4)$$

Along the radius direction and azimuth direction, the inner region of the current coil can be meshed into elements with total  $n = n_1 * n_2$ . The geometrical center of the  $ij$ th element is  $M_{ij}(x_{ij}, y_{ij}, 0)$ ,  $i=1,2,\dots,n_1, j=1,2,\dots,n_2$ .

Since the boat may pitch and roll during the navigation, the direction of the magnetic moment also changes accordingly. As indicated in Fig. 1 (c), the solenoid coil is axisymmetric and its orientation can be determined by  $\theta$  and  $\varphi$  in the global coordinate system. Then the sensor position is  $P(x,y,z) = G^{-1}P' + C$ ,  $G$  is the transition matrix and the magnetic flux density is derived as:

$$\mathbf{B} = \begin{bmatrix} B_x \\ B_y \\ B_z \end{bmatrix} = G^{-1} \mathbf{B}_d \quad (5)$$

$$= \begin{bmatrix} \cos \varphi & 0 & \sin \varphi \\ -\sin \theta \sin \varphi & \cos \theta & \sin \theta \cos \varphi \\ -\cos \theta \sin \varphi & -\sin \theta & \cos \theta \cos \varphi \end{bmatrix}^{-1} \mathbf{B}_d$$

### III. LOCALIZATION ALGORITHM BASED ON MULTI-OBJECTIVIZATION

#### A. Multi-objectivization

According to (4) and (5), the magnetic field  $\mathbf{B}$  generated by the circular coil is a high-order nonlinear function of the sensor position  $P(x,y,z)$  with 3 variables. The coil position  $C$  and the position angle  $\theta, \varphi$  can be obtained conveniently by the location equipment and gyroscopes in the survey boat. Then the localization of sensors is using the measured magnetic data  $\mathbf{B}_m$  to solve the inverse problem:

$$\begin{cases} \text{Minimize } \mathbf{f}(P) = (f_1(P), f_2(P), f_3(P))^T \\ f_1(P) = \|B_x - B_{mx}\|_2 \\ f_2(P) = \|B_y - B_{my}\|_2 \\ f_3(P) = \|B_z - B_{mz}\|_2 \end{cases} \quad (6)$$

Here,  $\mathbf{B}_m = [B_{mx} \ B_{my} \ B_{mz}]^T$  is the measured magnetic vector,  $\mathbf{B} = [B_x \ B_y \ B_z]^T$  is the calculated magnetic vector and  $\mathbf{f}(P)$  is the objective function vector. As shown in (6), the sensor position  $P$  can be determined by minimizing each objective

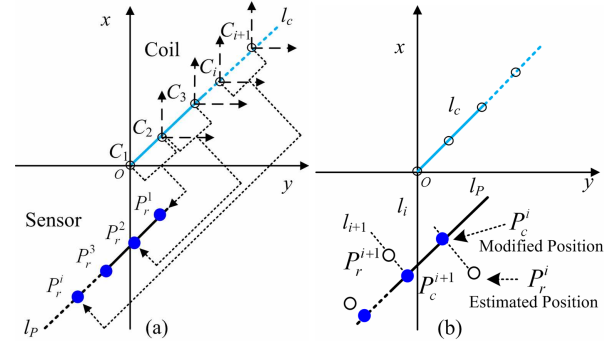


Fig. 2. Geometry for the Modification of the Estimated Positions by LMM.

function. For want of a better name, we call this three-objective model (TOM). The accuracy of localization can be improved with more objective functions, while it increases the time consumption. When the coil is placed in a different position, another measured magnetic vector will be collected. A six-objective model (SOM) can be defined as:

$$\text{Minimize } \mathbf{f}(P) = (f_1(B_{mx}^1), f_2(B_{my}^1), f_3(B_{mz}^1), f_4(B_{mx}^2), f_5(B_{my}^2), f_6(B_{mz}^2))^T \quad (7)$$

In order to correct the estimated positions, we apply a linear multi-metering method (LMM). As illustrated in Fig. 2 (a), we move the coil discontinuously from  $C_1$  to  $C_s$  along a straight line  $l_c$ , and then a set of magnetic field data is collected. The data is denoted as  $\mathbf{B}_m = [\mathbf{B}_m^1, \mathbf{B}_m^2, \dots, \mathbf{B}_m^s]^T$  ( $i=1,2,\dots,s$ ),  $\mathbf{B}_m^i = [B_{mx}^i, B_{my}^i, B_{mz}^i]^T$  is the measured magnetic vector when the coil is placed at location  $C_i$ . Subsequently, a series of SOMs are built by the adjacent data  $\mathbf{B}_m^i$  and  $\mathbf{B}_m^{i+1}$ . Obviously, we can obtain an array of the estimated sensor positions  $\mathbf{P}_r = [P_r^1, P_r^2, \dots, P_r^s]^T$  ( $i=1,2,\dots,s-1$ ) (Fig. 2 (a)).  $P_r^i$  is the estimated sensor position in the coil coordinates. As demonstrated in Fig. 2 (b), the estimated results might deviate from the trajectory. We use fitting method to correct the sensor position based on the reference line  $l_c$  and then obtain the corrected position  $P_c^i$ . Through conversion of coordinates, the modified sensor position can be expressed as:

$$P(x, y, z) = \frac{1}{s-1} \sum_{i=1}^{s-1} (G^{-1}P_c^i + C_i) \quad (8)$$

Generally, multi-objective optimization problem (MOOP) is simply converted into a single-objective optimization problem (SOOP) by weighted-sum method. Then the non-linear optimization approaches (e.g. LM method [20]-[22] and PSO [23]) are applied to minimize the fitness function iteratively. Nevertheless, the precision of the calculated position depends strongly on the initial position, which generally could not be given in real localization. Moreover, as we known, three components of the magnetic field generated by the coil vary with the position of a spatial point. It is hard to weight the relative importance of the objective functions and determine a valid set of weighted factors. Therefore, during the optimization approach it may not obtain satisfactory solutions due to the homogeneous magnetic field in a region.

Multi-objective optimization algorithms (MOOAs) simultaneously optimize all objective functions and require no initial guess and extra parameters. They can reduce the

effect of local optimal and increase search paths to the global optimum. Then a set of Pareto optimal solutions are obtained. As we multi-objectivize a SOOP, the global optimum of the original SOOP must be the most preferred solution of the Pareto optima [27].

In order to find the Pareto optima  $F$ , we use an improved variant of NSGA-II, which will be described in the next section. Then the most preferred solution in  $F$  can be determined by the following constrain:

$$\begin{cases} \text{Minimize } \text{fit}(P(x, y, z)) = \sum_{i=1}^m f_i(P(x, y, z)), \\ \text{s.t. } P(x, y, z) \in F \\ z > 0 \end{cases} \quad (9)$$

where  $m$  is the number of objectives,  $\text{fit}(P)$  is the summation function with respect to all objective values.

### B. An Improved Variant of NSGA-II

Evolutionary algorithms (EAs) have been found to be very useful in carrying out the optimization of multi-objective problem. NSGA firstly proposed by Srinivas and Deb in 1994[28]. It is a very effective algorithm but generally criticized for its computational complexity and non-elitism approach. It also requires the specification of a sharing parameter. Soon after, a fast elitist version, NSGA-II was developed by Deb et al. using a crowding distance measure and a front ranking method [29]. The runtime complexity of NSGA-II is  $O(gmN^2)$ .  $g$  is the maximum number of iterations,  $m$  and  $N$  are the number of objectives and the size of population, respectively. In order to reduce the run-time complexity, several modified versions of NSGA-II have been proposed [30]-[32]. A faster approach, NSGA-IIa, is suggested by trading off space against time in the sorting and ranking stage [33].

Fig. 3 (a) shows the sorting and ranking procedure of NSGA-IIa. The sorting of population ( $pop$ ) is performed based on each objective.  $Q_i$  represents the objective values of individuals sorted on the  $i$ th objective.  $I_i$  represents the index array of sorted population.  $S_q[I_i(j), i]$  returns the position( $pos$ ) of the  $I_i(j)$ th individual in the sorting based on the  $i$ th objective. During the sorting, the rank of each individual is assigned by summing up the position values in each objective.

As estimated in [33], the runtime complexity of NSGA-IIa is reduced to  $O(gmN \log_2 N)$ . However, the selection before mutation and crossover proceeds with respect to the assigned rank. It may not ensure the best individual based on each objective is propagated on to the next generation. Accordingly, we propose a hybridized approach using archive-based elitism and differential mutation (DE) [34] strategy to prevent the loss of good solutions for each objective. We call this variant the NSGA-IIb. The flowchart is given in Fig. 3 (b). After the sorting on  $i$ th objective, the individual  $G_i$  with best fitness value is selected for DE.

$$\begin{aligned} q_j &= p_j + v_1(G_i - p_j) + v_2(p_{r+1} - p_r) \\ (i &= 1, 2, \dots, m, j = 1, 2, \dots, N). \end{aligned} \quad (10)$$

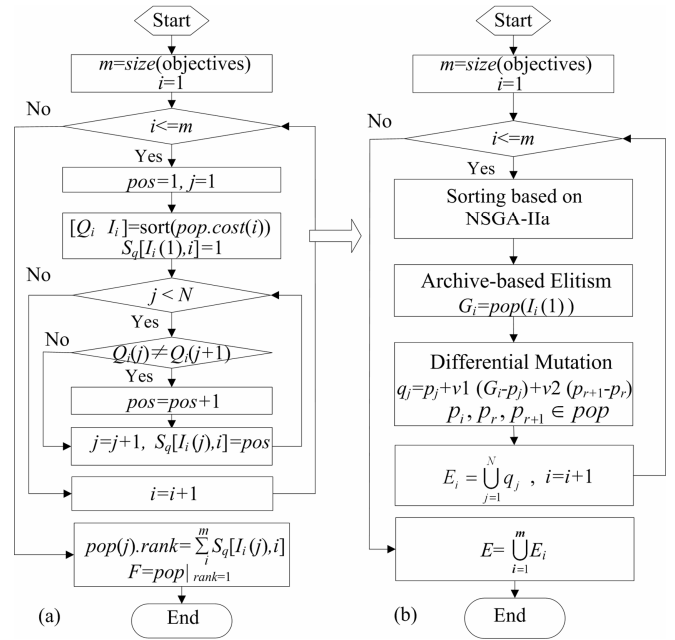


Fig. 3. Flowchart of (a) the Sorting and Ranking Scheme of NSGA-IIa, (b) Archive-based Elitism and Differential Mutation Strategy of NSGA-IIb.

where  $p_j$  is the parent individual,  $p_r$  and  $p_{r+1}$  are another two different parent individuals selected randomly.  $q_j$  is the offspring individual,  $v_1$  and  $v_2$  are the changing scale factors.

As indicated in (10), the variation  $(G_i - p_j)$  improves the convergence and the differential variation  $(p_{r+1} - p_r)$  increases the diversity of the offspring population. The greater the value of  $v_1$  is, the faster the algorithm converges, but the easier the algorithm traps in local optima. Comparatively, the greater the value of  $v_2$  is, the slower the algorithm converges, but the easier the algorithm finds global optima. Then  $v_1$  and  $v_2$  can be set respectively as:

$$\begin{cases} v_1 = v_{\max} - (v_{\max} - v_{\min})g_i / g, \\ v_2 = v_{\min} + (v_{\max} - v_{\min})g_i / g. \end{cases} \quad (11)$$

with  $v_{\max}$  the maximum scale factor,  $v_{\min}$  the minimum scale factor.  $g_i$  is the number of the current iteration. Usually, we let  $v_{\max}=0.9$ ,  $v_{\min}=0.3$ . Following the DE method, the best individuals for each objective and corresponding mutated individuals in population  $E$  are selected for the competition together with the new population, which are created by crossover and mutation in the main procedure.

## IV. EXPERIMENTS AND RESULTS

### A. Validation of the Discrete Model

In the numerical experiment, the coil is placed vertically at the origin  $C_1$ , and  $N_w=100$ ,  $R=0.045m$ ,  $I=2.5A$ . The main hardware configurations of computer are list as follows: CPU: Pentium(R) 2.8GHz, RAM: 2GB, and the software is Matlab7.1. There are 61\*121 sample points distributing in the  $x$ - $y$  plane with the spacing 0.01m. Here  $x \in [-0.3, 0.3]$ ,  $y \in [-0.6, 0.6]$ ,  $z=0.5$ .

We apply the explicit integral model (IM) and discrete model (DM) to calculate the magnetic flux density  $B$  at different spatial points, respectively. The calculation error is

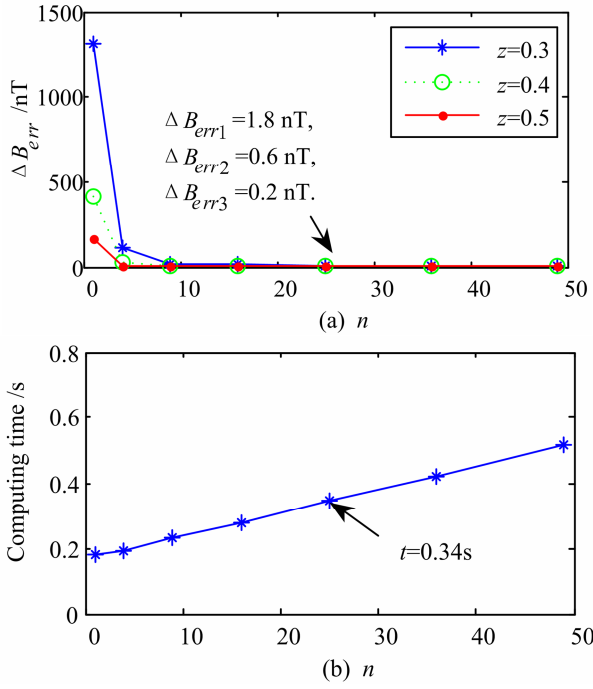


Fig. 4. Simulation results: (a) Calculation errors at different depths, (b) Computing time of DM.

defined as the maximum of the absolute error:  $\Delta B_{err} = |B_{IM} - B_{DM}|_{max}$ .

As indicated in Fig. 4(a), the calculation error  $\Delta B_{err}$  decreases rapidly with the number of the meshed elements  $n$ . The figure also clearly indicates the reducing errors for spatial points far from the coil. Fig. 4(b) shows the computing time of all the sample points using DM. Comparatively, the execution time of IM is 3.19s, which is much longer than that of DM. So it can be concluded that the discrete model of magnetic field generated by a current-carrying coil is accurate and less time-consumption.

### B. Localization Results

There are three parts in the experiment. Firstly, we evaluated the accuracy and execution time by applying different models of magnetic field and different multi-objective models based on NSGA-IIb. Secondly, we analyzed the influence caused by the measurement noise of the magnetic sensors and the deviation of the coil orientation. In the end, we carried out a mockup experiment. During the localization, an array of nine magnetic sensors was placed uniformly in the  $x$ - $y$  plane with size  $0.25 \times 0.3$ m and  $z=0.514$ m. Then the coil moved through the sensor area along the central line. In the process of optimization, the population size is set as  $N=500$ , and the number of iterations  $g=15$ , the number of the meshed elements  $n=25$ . The position errors are defined as follows:

$$d_r = \sqrt{(x-x_0)^2 + (y-y_0)^2 + (z-z_0)^2}, \quad R_e = d_r / r. \quad (12)$$

Here,  $d_r$  is the distance error between the estimated position  $P(x,y,z)$  and the true position  $P_0(x_0,y_0,z_0)$ ,  $r$  is the distance between the sensor and the coil,  $R_e$  is the relative error.

Fig. 5(a) and (b) show the position errors when different multi-objective models (TOM and SOM) and magnetic field models (DM and IM) are applied based on NSGA-IIb.

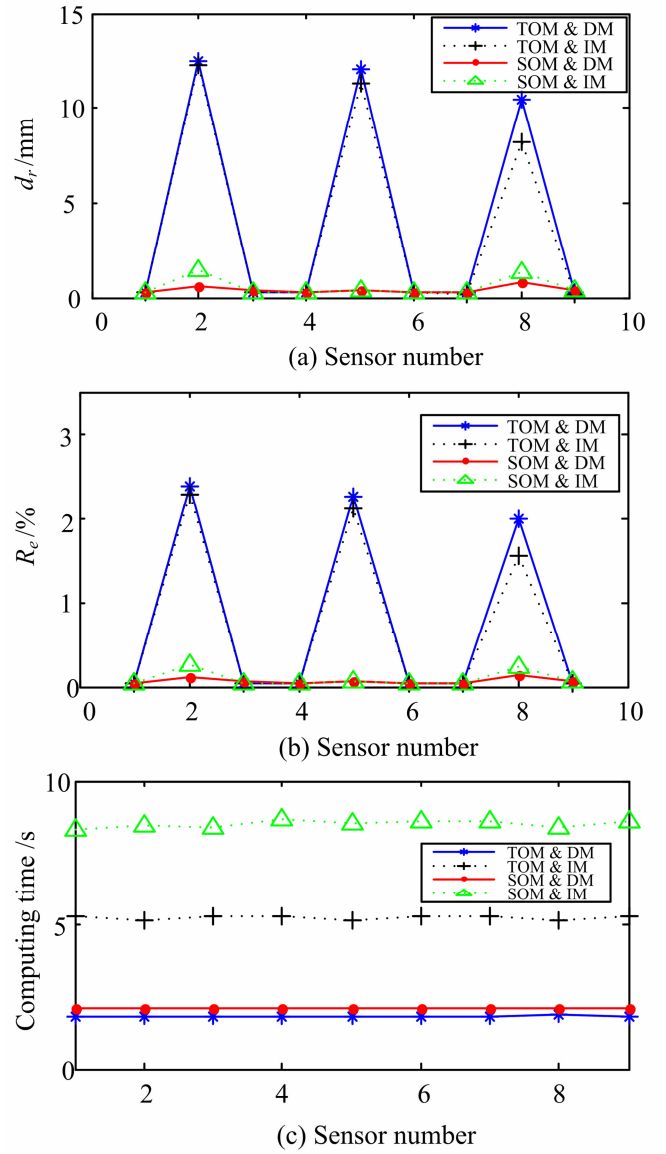


Fig. 5. Localization Results Using Different Models.

Obviously, the position errors of SOM are much smaller than that of TOM, while the position errors of DM are comparable with that of IM. Fig. 5(c) indicates that the execution time of IM is four times as long as that of DM. Accordingly, the method using SOM and DM are preferable, which lead to a more localization of the sensors with satisfactory accuracy. The average position errors of the sensor array are  $d_r=0.4$ mm,  $R_e=0.06\%$ . The average time is about 2.13s, which is much fewer than that in [23] by PSO ( $2.2s \times 3$ ).

In order to examine the robustness of the proposed method, firstly, we introduced measurement noise of different signal-to-noise ratio (SNR) in each sensor. Table I shows the average position errors and the maximum position errors of the sensor array for various measurement noises. We observe that the localization errors of SOM and LMM are small ( $d_r < 4.2$ mm,  $R_e < 1\%$ ) when SNR is larger than 15 dB. Compared with SOM, the localization accuracy is improved by LMM. Since the moving boat may pitch and roll in the offing, we consider a random measurement error of the coil orientation.  $(\Delta\theta, \Delta\varphi)$  is the maximum of the orientation deviation of the coil. Table II shows that the average distance



TABLE I  
POSITION ERROR FOR MEASUREMENT NOISE OF THE SENSORS

SNR(dB)	SOM			
	$d_r$ -max	$d_r$ -average	$R_e$ -max	$R_e$ -average
5	55.85	33.68	8.29	4.93
10	32.01	13.01	3.76	1.82
15	4.12	3.10	0.59	0.46
20	2.22	1.27	0.41	0.20

SNR(dB)	LMM			
	$d_r$ -max	$d_r$ -average	$R_e$ -max	$R_e$ -average
5	14.02	10.32	2.25	1.65
10	9.36	3.74	1.50	0.60
15	1.86	0.88	0.30	0.14
20	0.60	0.32	0.10	0.05

TABLE II  
POSITION ERROR FOR DEVIATION OF THE COIL ORIENTATION

$(\Delta\theta, \Delta\varphi)$ ( $^\circ$ )	SOM			
	$d_r$ -max	$d_r$ -average	$R_e$ -max	$R_e$ -average
(1.0,1.0)	10.26	4.50	1.25	0.60
(3.0,3.0)	18.71	12.55	2.44	1.77
(5.0,5.0)	32.06	22.91	4.53	3.20
(7.0,7.0)	49.06	33.56	6.59	4.75

$(\Delta\theta, \Delta\varphi)$ ( $^\circ$ )	LMM			
	$d_r$ -max	$d_r$ -average	$R_e$ -max	$R_e$ -average
(1.0,1.0)	5.43	1.90	0.87	0.30
(3.0,3.0)	5.67	3.91	0.91	0.63
(5.0,5.0)	12.63	5.44	2.03	0.87
(7.0,7.0)	16.90	9.92	2.71	1.59

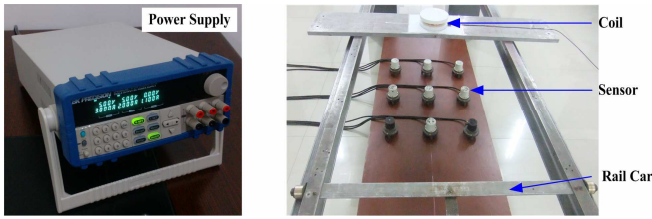


Fig. 6. The Experimental Setup for Localization of the Magnetic Sensor Array.

error by LMM is less than 5.5mm and the relative error is less than 1% when  $\Delta\theta$  and  $\Delta\varphi$  are smaller than  $5^\circ$ . It means that the measurements of  $\theta$  and  $\varphi$  are unnecessary if the orientation angles of the coil are small. According to Tables I and II, it is evident that the hybrid algorithm using NSGA-IIb and LMM has satisfactory accuracy and strong robustness.

As shown in Fig. 6, a mockup experiment is carried out. The power equipment has a resolution 1mA, a range 0~6A and current ripple is less than 6mArms. It supplies a direct current for the circular coil, which is carried by a non-magnetic rail car. The magnetic sensors have a resolution 1nT and a range  $\pm 60\mu T$ . When the coil moves to a predetermined position, nine uniformly arranged sensors measure the magnetic field simultaneously. In the experiment, the coil is place vertically and the orientation of the coil is  $\theta = \varphi = 0$ . Fig. 7 shows the localization results by SOM and LMM. Obviously, LMM has better localization accuracy than SOM. The average distance error of the sensor array by LMM is about 11.67mm, and the average relative error is about 1.87%. Compared to another study [24] ( $R_e=12.9\%$ ), the proposed method shows preferable accuracy for the localization of the magnetic sensor.

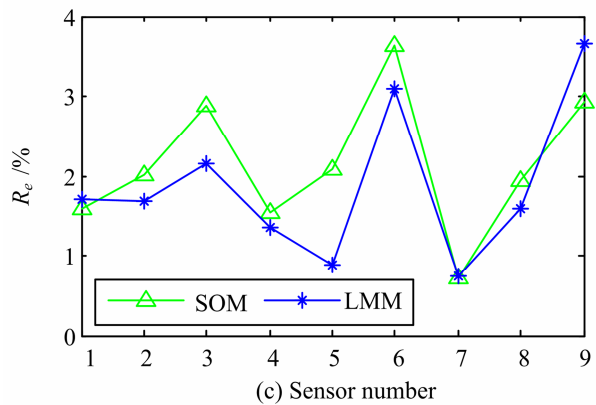
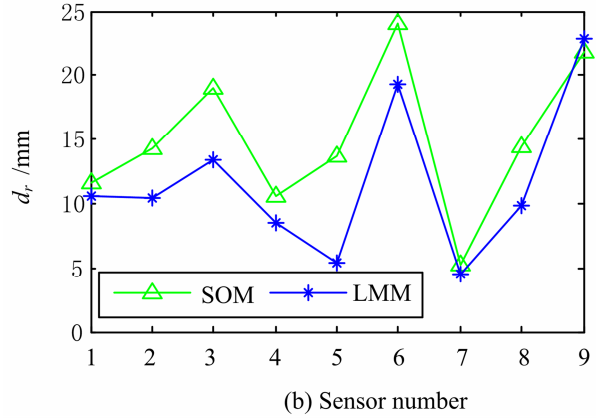
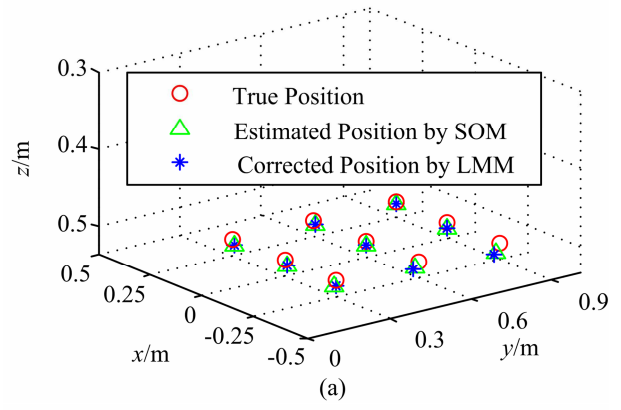


Fig. 7. Localization Results of the Mockup Experiment.

## V. CONCLUSIONS

A hybrid algorithm based on multi-objectivization has been proposed to localization the underwater sensor networks. The DC coil serves as a magnetic source, and it follows a predetermined trajectory. Then using the three-component magnetic data measured by the triaxial magnetometer in the sensor, the localization problem is converted into a multi-objective optimization problem. Compared to the explicit integration, the discrete model of magnetic field considerably decreases the time consumption during the optimization. The experiment results show that the proposed localization algorithm using improved Non-dominated Sorting Genetic Algorithm (NSGA-IIb) and linear multi-metering (LMM) is effective. Its high accuracy and strong robustness also has been validated. During the experiment, the imperfect circular shape and the thickness of the coil cause errors in the localization results. In the future, we intend to reduce error by improving magnetic field model and the correction method, and then apply the proposed

algorithm in a real localization system.

# ACKNOWLEDGMENT

This project is supported by the National Natural Science Foundations of China (51107145 and 51377165).

# REFERENCES

- [1] V. Chandrasekhar, W. K. Seah, Y. S. Choo, and H. V. Ee, "Localization in underwater sensor networks, survey and challenges," in *Proc. 1st Conf. Works. Unde. Netw.*, Los Angeles, USA, 2006, pp.33–40.
- [2] M. Erol-Kantarci, H. T. Mouftah, and S. Oktug, "A Survey of Architectures and Localization Techniques for Underwater Acoustic Sensor Networks," *IEEE Commun. Surv. & Tutor.*, vol. 13, no. 3, pp. 487–502, Nov. 2011.
- [3] M. J. Partan, J. Kurose, and B. N. Levine, "A survey of practical issues in underwater networks," in *Proc. 1st Conf. Works. Unde. Netw.*, Los Angeles, USA, Oct. 2006, pp. 17–24.
- [4] D. H. Shin, and T. K. Sung, "Comparisons of error characteristics between TOA and TDOA Positioning," *IEEE Trans. Aerosp. Electron. Syst.*, vol. 38, pp. 307–311, Jan. 2002.
- [5] K. Whitehouse, C. Karlof, and D. Culler, "A practical evaluation of radio signal strength for ranging-based localization," *Sigmobile Mob. Comput. Commun. Rev.*, vol. 11, pp. 41–52, Jan. 2007.
- [6] D. Niculescu, and B. Nath, "Ad Hoc Positioning System (APS) Using AOA," in *Proc. IEEE Infocom.*, San Francisco, CA, USA, Apr. 2003, pp. 1734–1743.
- [7] M. Cedervall, and R. L. Moses, "Efficient maximum likelihood DOA estimation for signals with known waveforms in the presence of multipath," *IEEE Trans. Signal Proc.*, vol. 45, pp. 808–811, Mar. 1997.
- [8] T. He, C. Huang, B. Blum, J. A. Stankovic, and T. Abdelzaher, "Range-free localization schemes in large scale sensor networks," in *Proc. 9th ACM Mobi. Com.*, New York, NY, USA, Sep. 2003, pp. 81–95.
- [9] N. B. Priyantha, H. Balakrishnan, E. Demaine, and S. Teller, "Mobile-Assisted Localization in Wireless Sensor Networks," in *Proc. IEEE Conf. Comp. Comm.*, Miami, FL, USA, Mar. 2005, pp.172–183.
- [10] V. Chandrasekhar, and W. Seah, "An area localization scheme for underwater sensor networks," in *Proc. IEEE Oceans Asia Pacif. Conf.*, Singapore, May 2007, pp. 1–8.
- [11] S. Lee, and K. Kim, "Localization with a Mobile Beacon in Underwater Sensor Networks," in *Proc. IEEE 8th Inter. Conf. Embe. Ubiqu. Comp.*, Hong Kong, China, Dec. 2010, pp. 316–319.
- [12] M. Erol-Kantarci, H. T. Mouftah, and S. Oktug, "Localization techniques for underwater acoustic sensor networks," *IEEE Commun. Mag.*, vol. 48, pp. 152–158, Dec. 2010.
- [13] G. Han, J. Jiang, L. Shu, Y. Xu, and F. Wang, "Localization Algorithms of Underwater Wireless Sensor Networks: A Survey," *IEEE Sensors*, vol. 12, no. 2, pp. 2026–2061, Feb. 2012.
- [14] H. Luo, Z. Guo, W. Dong, F. Hong, and Y. Zhao, "LDB: Localization with directional beacons for sparse 3D underwater acoustic sensor networks," *J. Netw.*, vol. 5, pp. 28–38, Jan. 2010.
- [15] M. Erol, L. Vieira, and M. Gerla, "Localization with Dive-N-Rise (DNR) beacons for underwater acoustic sensor networks," in *Proc. 2nd works. Unde. Netw.*, Montreal, Quebec, Canada, Sep. 2007, pp. 97–100.
- [16] X. Cheng, H. Shu, Q. Liang, and D. H. Du, "Silent positioning in underwater acoustic sensor networks," *IEEE Trans. Vehicul. Technol.*, vol. 57, pp. 1756–1766, May. 2008.
- [17] A. Sheinker, L. Frumkis, B. Ginzburg, N. Salomonski, and B. Kaplan, "Magnetic Anomaly Detection Using a Three-Axis Magnetometer," *IEEE Trans. Mag.*, vol. 45, pp. 160–167, Jan. 2009.
- [18] N. Wahlstrom, J. Callmer, and F. Gustafsson, "Magnetometers for tracking metallic targets," in *Proc. 13th Conf. Infor. Fusi.*, EICC, Edinburgh, UK, Jul.2010, pp.1–8.
- [19] A. V. J. Kildishev, A. Nyenhuis, and M. A. Morgan, "Multipole analysis of an elongated magnetic source by a cylindrical sensor array," *IEEE Trans. Mag.*, vol. 38, pp. 2465–2467, Sep. 2002.
- [20] C. Hu, M. Li, S. Song, W. Yang, R. Zhang, and M. Q. H. Meng, "A Cubic3-Axis Magnetic Sensor Array for Wirelessly Tracking Magnet Position and Orientation," *IEEE Sensors.*, vol. 10, pp. 903–913, May 2010.
- [21] V. Schlageter, P. A. Besse, R. S. Popovic, and P. Kucera, "Tracking system with five degrees of freedom using a 2D-array of Hall sensors

and a permanent magnet," *Sens. Actuators A: Phys.*, vol. 92, pp. 37–42, Aug. 2001.

- [22] X. Wu, W. Hou, C. Peng, X. Zhen, X. Fang, and J. He, "Wearable magnetic locating and tracking system for MEMS medical capsule," *Sens. Actuators A: Phys.*, vol. 141, pp. 432–439, Feb. 2008.
- [23] W. Yang, C. Hu, M. Li, M. Q. H. Meng, and S. Song, "A New Tracking System for Three Magnetic Objectives," *IEEE Trans. Mag.*, vol. 46, pp. 4023–4029, Dec. 2010.
- [24] J. Callmer, M. Skoglund, and F. Gustafsson, "Silent localization of underwater sensors using magnetometers," *Eurasip J. Adv. Sig. Proc.*, 2010, 1–8.
- [25] Z. Zhang, and C. Xiao, "Simulation Experiment Research for Magnetic Localization Method for Magnetometer Sensor at Seabed," *Jour. Shanghai Jiaotong Univer.*, vol. 45, no. 6, pp. 826–829, Jun. 2011.
- [26] G. Lehner, "Basics of Magnetics," in *Electromagnetic Field Theory for Engineers and Physicists*, 1sted., M. Horrer, Ed. Berlin: Springer, 2010, pp. 256–283.
- [27] J. D. Knowles, R. A. Waston, and D. W. Corne, "Reducing local optima in single-objective problems by multi-objectivization," in *1st Conf. Evolu. Multi-Criterion Optim.*, Zurich, Switzerland, Mar. 2001, pp.7–9.
- [28] N. Srinivas, and K. Deb, "Multiobjective Optimization Using Non-dominated Sorting in Genetic Algorithms," *Evol. Comput.*, vol. 2, pp. 221–248, Dec. 1994.
- [29] K. Deb, A. Pratap, S. Agarwal, and T. Meyarivan, "A fast elitist multi-objective genetic algorithm: NSGA-II," *IEEE Trans. Evol. Comput.*, vol. 6, pp. 182–197, Apr. 2002.
- [30] M. T. Jensen, "Reducing the run-time complexity of multiobjective EAs: The NSGA-II and other algorithms," *IEEE Trans. Evol. Comput.*, vol. 7, pp. 503–515, Oct. 2003.
- [31] H. Fang, Q. Wang, Y. Tu, M. F. Horstemeyer, "An efficient non-dominated sorting method for evolutionary algorithms," *IEEE Trans. Evol. Comput.*, vol. 16, pp. 355–384, Spe. 2008.
- [32] K. D. Tran, "An Improved Non-dominated Sorting Genetic Algorithm-II (ANSGA-II) with adaptable parameters," *Intl. J. Intel. Syst. Tech. Appl.*, ol., vol. 7, pp. 347–369, Spe. 2009.
- [33] R. G. L. D'Souza, K. C. Sekaran, and A. Kandasamy, "Improved NSGA-II Based on Novel Ranking Scheme," *J. Comput.*, vol. 2, pp. 91–95, Feb. 2010.
- [34] R. Storn, and K. Price, "Differential Evolution- A Simple and Efficient Heuristic for Global Optimization over Continous Spaces," *J. Global Optimization*, vol. 11, pp. 341–359, Dec. 1997.



Zhou Yu received a B.S. in automation from Huazhong University of Science and Technology, Wuhan, China, in 2007 and awarded his M.S. in control theory and engineering from Navy University of Engineering in 2009. He is currently pursuing a Ph.D. in electrical engineering at Navy University of Engineering with interest in magnetic sensors, underwater sensor networks, magnetic measurement techniques and magnetic localization.

Changhan Xiao received the M.S. degree in astrophysics from Huazhong Normal University, Wuhan, China, and a Ph.D. degree in electrical engineering from Huazhong University of Science and Technology in 1995 and 1998. He is currently a Professor in the College of Electrical Engineering at Naval University of Engineering. His researches are in the area of mathematical physics, engineering electromagnetics, intelligent instrumentation and ferromagnetism.



Guohua Zhou received his M.S. degree and Ph.D. degree in electrical engineering from the Navy University of Engineering, in 2005 and 2009, respectively. After graduation he stayed with Changhan Xiao and now he is a senior researcher. His research activities include electromagnetic computation, optimization techniques. He has roughly published 30 refereed journal articles and is responsible for a National Natural Science Foundation of China.

